• Basic Research •

Biosafety of a 3D-printed intraocular lens made of a poly(acrylamide-co-sodium acrylate) hydrogel *in vitro* and *in vivo*

Jia–Wen Li[1,2], Yi–Jian Li[1,2], Xi-Su Hu[1,2], Yu Gong[1,2], Ben–Bin Xu[3], Hai–Wei Xu[1,2], Zheng–Qin Yin[1,2]

[1]Southwest Hospital/Southwest Eye Hospital, Third Military Medical University (Army Medical University), Chongqing 400038, China

[2]Key Lab of Visual Damage and Regeneration & Restoration of Chongqing, Chongqing 400038, China

[3]Smart Materials and Surfaces Lab, Faculty of Engineering and Environment, Northumbria University, Newcastle upon Tyne NE1 8ST, UK

Correspondence to: Hai-Wei Xu and Zheng-Qin Yin. Southwest Hospital/Southwest Eye Hospital, Third Military Medical University (Army Medical University), Chongqing 400038, China. xuhaiwei@tmmu.edu.cn; qinzyin@aliyun.com
Received: 2020-01-23   Accepted: 2020-07-10

Abstract

● **AIM:** To assess the biosafety of a poly(acrylamide-co-sodium acrylate) hydrogel (PAH) as a 3D-printed intraocular lens (IOL) material.

● **METHODS:** The biosafety of PAH was first evaluated *in vitro* using human lens epithelial cells (LECs) and the ARPE19 cell line, and a cell counting kit-8 (CCK-8) assay was performed to investigate alterations in cell proliferation. A thin film of PAH and a conventional IOL were intraocularly implanted into the eyes of New Zealand white rabbits respectively, and a sham surgery served as control group. The anterior segment photographs, intraocular pressure (IOP), blood parameters and electroretinograms (ERG) were recorded. Inflammatory cytokines in the aqueous humor, such as TNFα and IL-8, were examined by ELISA. Cell apoptosis of the retina was investigated by TUNEL assay, and macroPAHge activation was detected by immunostaining.

● **RESULTS:** PAH did not slow cell proliferation when cocultured with human LECs or ARPE19 cells. The implantation of a thin film of a 3D-printed IOL composed of PAH did not affect the IOP, blood parameters, ERG or optical structure in any of the three experimental groups (*n*=3 for each). Both TNFα and IL-8 in the aqueous humor of PAH group were transiently elevated 1wk post-operation and recovered to normal levels at 1 and 3mo post-operation. Iba1^{+} macroPAHges in the anterior chamber angle in PAH group were increased markedly compared to those of the control group; however, there was no significant difference compared to those in the IOL group.

● **CONCLUSION:** PAH is a safe material for 3D printing of personal IOLs that hold great potential for future clinical applications.

● **KEYWORDS:** cataract; biosafety; lens epithelial cells; ARPE19 cells; intraocular lens; 3D printing; poly hydrogel; rabbit

INTRODUCTION

More than 95 million people worldwide have cataracts, which is the leading cause of blindness[1]. PAHcoemulsification combined with intraocular lens (IOL) implantation is the most effective way to treat cataract so far[2]. However, the mass-produced model IOL based on a high-precision machine tool fails to meet the growing demands of personalized customization of the human lens, and it is hard to obtain the best postoperative vision[3]. Precision medicine is an inevitable trend in the development of clinical medicine, personalized customization is an extremely important component of precision medicine, and personalized IOL customization is an important means to improve the outcome of cataract surgery.

3D printing holds great potential in biomedical engineering research as well as in ophthalmologic applications[4-6], which enables cost-effective products and instruments that aid in therapeutic devices, such as IOLs, built specifically for individual cataract patients[7]. Based on the clinical data, it is possible for us to design a personalized IOL suitable for the size of the lens capsule by digital optical modeling, simulating the quality of IOL imaging and correcting the wave front aberration[7]. Achievement of 3D printing of IOLs is a great challenge, and the breakthrough bottleneck lies in

the following points: 1) the fabrication of ultrahigh-precision roughness of the IOL surface (micro/nano-precision)[8]; 2) the high transparency and UV-blocking ability of materials; 3) the flexibility, water richness and micromechanical characteristics of the organic materials; and 4) the biosafety of the material for 3D-printed IOLs[9-10].

Additive manufacturing and 3D printing create new approaches for the design and manufacturing of implants, such as micro-structured eye implants, including multifocal diffractive aspheric IOL[11]. We planned to print the IOL mold with a new responsive poly(acrylamide-co-sodium acrylate) hydrogel (PAH) with 3D precise printing technology, which aims to provide accurate and personalized IOL products for cataract patients. The gel is a fully diluted crosslinking system that has no fluidity in the stable state. The main component of the gel is liquid by weight. However, due to the 3D crosslinking network, the structural integrity of the hydrogel network will not be dissolved due to the high hydrophilicity. Hydrogels are highly absorbent and light permeable (containing more than 90% water). Due to its high-water content, the hydrogel also has a very similar flexibility to natural tissue, which makes it an ideal 3D printing material for making personalized IOLs. However, as responsive smart materials, hydrogels can encapsulate chemical compounds such as glucose, which are released by the stimulation of external factors, such as changes in pH. Thus, whether a PAH is toxic to ocular tissue needs to be deliberately considered. Nevertheless, the issue of the biosafety of PAHs is unclear so far.

Here, we utilized a PAH to create a thin film in order to investigate its biosafety after intraocular implantation. It was demonstrated *in vivo* that intraocular pressure (IOP), electroretinograms (ERGs) and inflammatory factors in the aqueous humor exhibited no significant difference after PAH implantation. Moreover, similar results could be verified by experiments *in vitro*. Taken together, the results indicate that the PAH does not harm the rabbit ocular tissue and causes no inflammation *in vitro* or *in vivo*, supporting the idea that it is a safe material for on-demand manufacturing of patient-personalized IOLs.

MATERIALS AND METHODS

Ethical Approval All animal experimental procedures were formally approved by the Institutional Review Board of the Army Medical University and adherence to the ARVO Statement for the Use of Animals in Ophthalmic and Vision Research.

Laboratory Animal Welfare All experiments were performed on New Zealand white rabbits provided by the Experimental Animal Centre of Southwest Hospital, Army Medical University. The New Zealand white rabbits were all raised in the Animal Care Centre of the Army Medical University and maintained with free access to water and food under a 12-h light/dark cycle.

Preparation of the PAH Thin Film The hydrogel solution was prepared according to the following formula: 17.5% N-isopropylacrylamide; 12.5% sodium acrylate; 1.5% N,N'-methylenebisacrylamide; N,N,N',N'-tetramethylethylenediamine; 10% ammonium persulfate, H_2O. The solution was added to one of the molds and immediately joined with another mold. Then, the two pieces of mold were clamped together. After 30-60min, the gel was solidified, and the two molds were removed. The formed hydrogel crystals were transferred to phosPAHte buffered saline (PBS) for preservation.

Intraocular Implantation of the PAH Thin Film into New Zealand White Rabbit Eyes The New Zealand white rabbits were divided into three groups based on implants: the PAH thin film as the hydrogel group, the conventional IOL as the IOL group, and the sham surgery as the control group (*n*=3 for each group). Animals were anesthetized with 3% pentobarbital sodium 1 mL/kg through the ear-rim auricular vein; the left eye was selected as the operative eye. Before the operation, tropicamide eye drops (Santen) were used for mydriasis. The eyelid was opened with an eye speculum, and the conjunctival sac was soaked with 5% povidone iodine for 90s and then rinsed with saline. A 3.0-mm width transparent corneal incision was made at the 12 o'clock position, a 1.0-mm width auxiliary corneal incision was made at the 9 o'clock position, and sodium hyaluronate (SINGCLEAN) was injected into the anterior chamber. For the control group, the incision was sutured directly with 10-0 polypropylene. For the hydrogel group and IOL group, we performed capsulorhexis, water separation, and PAHcoemulsification of the lens nucleus (Laureate, Alcon, USA), cleared the lens cortex with I/A, and injected the PAH thin film (5 mm×5 mm) or IOL (860 UV, acrylic intraocular lenses as a positive control of biosafety). The 12 o'clock incision was sutured with 10-0 nylon suture, balanced salt solution (BSS) was injected to form the anterior chamber capacity, and tobramycin dexamethasone eye ointment (Alcon, USA) was applied to the eyes after the operation. IOP was measured by a noncontact tonometer at 1d, 1wk, 1, and 3mo post-operation.

Euthanasia and Histopathology Three months after implantation, the New Zealand white rabbits were euthanized with pentobarbital sodium (400 mg/kg) administered intravenously. Afterwards, each eye containing the implant was taken from each rabbit for histological examination. Specimens were fixed in 4% paraformaldehyde for at least 24h and dehydrated in 30% sucrose for at least 24h, followed by embedding with Tissue-Tek O.C.T. Compound (Sakura Finetek USA, Inc., Torrance, CA 90501, USA). All tissue

pieces were cut into 2-4 µm thick tissue sections (Leica CM1900UV cryostat). Then, all sections were routinely stained with hematoxylin-eosin (HE) and examined under a light microscope (OLYMPUS DP71; Olympus Europa SE & Co. KG, Hamburg, Germany) to assess fibroblast proliferation and anatomical abnormalities.

Cell Culture Human lens epithelial cells (LECs) were expanded from lens explants, which were provided by the Southwest Hospital Eye Bank. Briefly, the lens was washed in cold PBS containing 50 U/mL penicillin and 100 µg/mL streptomycin, cut into 5 mm×5 mm small pieces and seeded onto human vitronectin (Gibco, Thermo Fisher, USA) precoated plates, and the explants were left for attachment. The second day, LECs were cultured in conditioned medium consisting of DMEM/F12 (HyClone), 10% FBS (Gibco), insulin-transferrin sodium selenite (1 µg/mL, Gibco), penicillin (100 U/mL) and streptomycin (100 µg/mL, HyClone). As cells reached subconfluence, they were gently passaged at 1:6 to expand. The ARPE19 cell line was cultured according to the same procedures and conditions described above. The cells were co-cultured with the PAH thin film (5 mm×5 mm) or PBS as control.

Immunostaining to Identify LECs Immunostaining was routinely performed as previously described[12]. Sections were incubated for 15min with PBS, and sections were further incubated with PBS containing 0.1% (vol/vol) Triton X-100 for 15min and further blocked with 1% (wt/vol) bovine serum albumin (BSA) in PBS at room temperature. The following primary antibodies were incubated at 4℃ overnight: Pax6 (1:500, Abcam), Sox2 (1:400, Abcam), αA-crystallin (1:200, Santa Cruz), α-SMA (1:400, Abcam), and Iba1 (1:500, Wako).

TUNEL Staining to Analyze the Apoptotic Cells and Immuno Cells in the Eyes of Rabbits Using the TUNEL Assay Kit (Abcam) as previously described[13], the secondary antibodies included the goat anti-mouse Alexa Fluor 488 and goat anti-mouse Alexa Fluor 594 (Invitrogen). DAPI (1:10, Beyotime) was incubated for 8-10min at 20℃ to counterstain nuclei, followed by cover-slipping with antifade mounting medium (Beyotime).

CCK-8 Assay to Analyze the Proliferation of LECs and APRE19 Cells The cytotoxicity of the PAH was measured using the Cell Counting Kit-8 (CCK-8) assay according to a previously published protocol[14]. Absorbance at wavelengths of 450 and 650 nm was collected using a microplate reader (Varioskan Flash, Thermo Fisher, USA).

ELISA Assay to Analyze Cytokines The aqueous humor was extracted with a 30 G sterile needle syringe at the 9 o'clock position of the limbus at 1wk, 1, and 3mo post-operation. ELISAs to detect IL-8 and TNF (cloud-clone corp.) were performed as previously reported[15]. The absorbance of each well was read at 450 and 550 nm. The 550 nm values were subtracted from the 450 nm values to correct for optical imperfections in the microplate.

Electroretinogram Recording to Assess The Visual Function of Rabbits Scotopic flash ERG recording was performed at 3mo post-operation as described previously[16]. Briefly, after 12-h dark adaptation, the rabbits were carefully anesthetized with 3% pentobarbital sodium (1 mL/kg). The pupils were dilated with 1% tropicamide. The body temperature was maintained at 37℃ with a heating pad to prevent hypothermia. Active gold electrodes were placed onto cornea serving as the recording electrodes. The reference and ground electrodes were placed subcutaneously in the mid-frontal areas of the head and back, respectively. We performed light stimulation at densities of -2.5, -0.5, -0.02, and 0.5 log $(cd·s/m^2)$ for New Zealand white rabbits and 0.5 log $(cd·s/m^2)$ for rabbits. The amplitudes and peak times of the a-waves and b-waves were recorded and processed through a RETI-Port device (Roland Consult). All experimental procedures were performed in a dark room under dim red safety light.

Microscopy, Image Acquisition, and Processing All confocal images were collected by a Zeiss LSM880. Immunostaining data were all processed in Image J and Illustrator (Adobe).

Statistical Analysis Data are shown as the means±standard deviation (SD). All statistical tests were performed by PRISM (GraphPad). Statistical significance was detected by Student's t-test (parametric). A $P<0.05$ was considered statistically significant.

RESULTS

Synthesis of the PAH To produce patterned morphology and structure, a precise 3D-printed IOL mold was injected into the new responsive PAH (Figure 1A). To better adapt for implantation into rabbit eyes, a thin film-like PAH was made (Figure 1B). As a fresh hydrogel often remains unstable and releases small molecular chemical compounds such as glucose, to achieve a stable state of the PAH, we pretreated the hydrogel with PBS and examined its optimal condition to reduce the influence on LECs. We found that after 9d of pretreatment with PBS, the PAH did not affect the survival or proliferation of LECs (Figure 1C, 1D).

Effect of the PAH on LECs and ARPE19 Cells *In Vitro* To investigate whether the PAH disturbs cell viability, we cocultured the PAH with LECs and ARPE19 cells. The cultured cells positively expressed LEC markers, such as PAX6 and SOX2, and synthesized the specific a-A crystallin and negatively expressed the fibroblast cell marker a-SMA, which identified the LECs (Figure 2A-2F). When LECs were cocultured with the PAH, cell apoptosis emerged only at the adjacent area around the hydrogel (Figure 2G, 2H). A similar result could be obtained when it cocultured with ARPE19 cells.
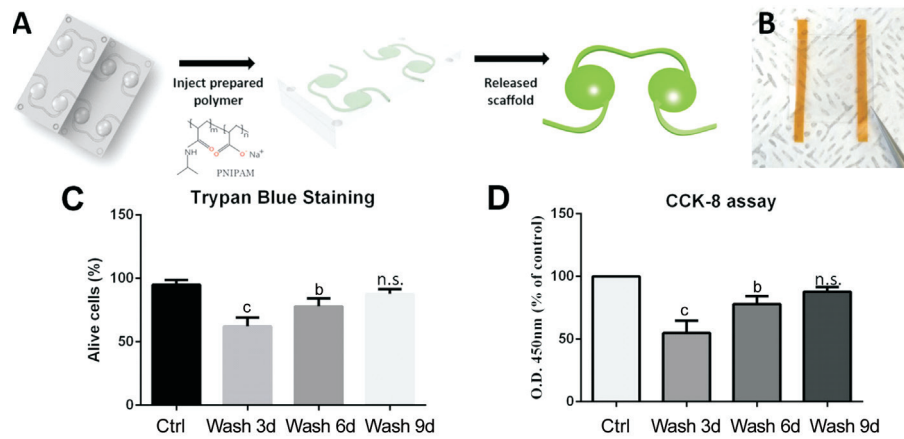
Figure 1 Synthesis of the PAH thin film A: A precise 3D-printed IOL mold was injected into the new responsive PAH to produce a patterned morphology and structure; B: Image of the PAH thin film; C: Trypan blue staining of LECs co-cocultured with the PAH at 0, 3, 6, and 9d of the PBS wash; D: CCK-8 assay of LECs co-cocultured with the PAH at 0, 3, 6, and 9d of the PBS wash. Data are shown as the mean±SD. $^bP<0.01$, $^cP<0.005$. n.s.: No significance. Independent sample t-test.
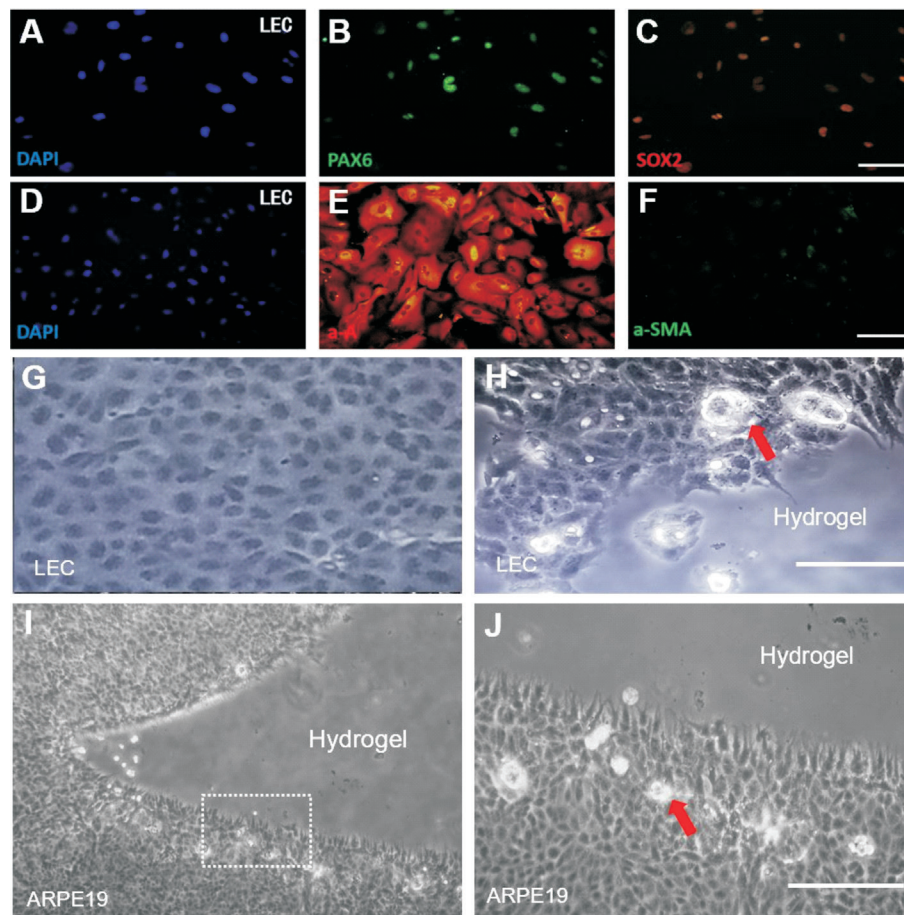

Figure 2 Coculture of PAH thin films with LECs or ARPE19 cells A-F: Immunostaining of LECs showed that LECs were positively stained for the LEC markers PAX6 (A, B), SOX2 (C), and α-A crystallin (D, E) and negatively stained for the fibroblast cell marker α-SMA (F); G-H: Bright field images of LECs co-cultured with (H) or without (G) the PAH. Cells adjacent to the hydrogel were unable to attach to the matrix and ultimately underwent apoptosis (red arrow). I-J: Bright field images of ARPE19 cells co-cultured with the PAH (I). The magnified image (J, white dashed area in I) shows that a minority of adjacent cells underwent cell apoptosis (red arrow), whereas the distal cells stayed in a normal proliferative state. Scale bar: 50 μm (A-F), 100 μm (G-J).

Biosafety of PAH Implantation into Anterior Chamber
To further evaluate the biosafety of PAHs, we performed intraocular implantation in New Zealand white rabbits. Slit-lamp imaging at 1wk post-operation indicated corrected location of the hydrogel at the anterior chamber (Figure 3A-3C). No significant corneal opacification, keratic precipitate,
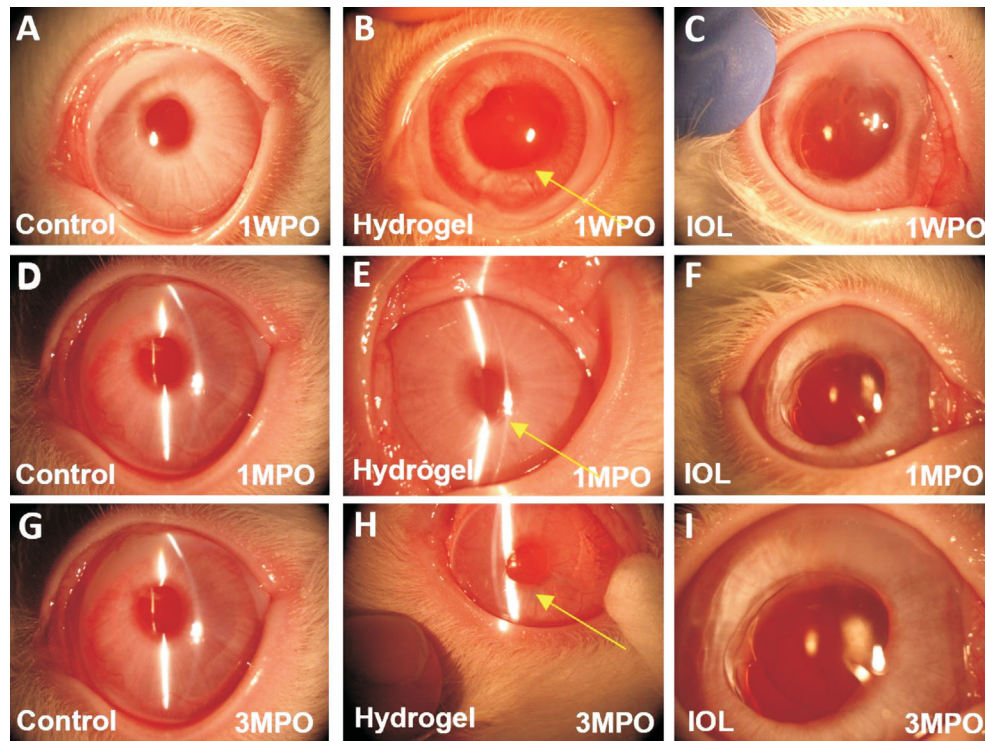
Figure 3 Implantation of PAH thin film into the anterior chamber of New Zealand white rabbits does not induce endophthalmitis A-C: Slit lamp images of the control group (A), hydrogel group (B) and IOL group (C) at 1wk post-operation showed successful implantation and correct location of the implants; D-F: Slit lamp images of the control group (D), hydrogel group (E) and IOL group (F) at 1mo post-operation showed no significant corneal opacification, keratic precipitate or endophthalmitis; G-I: Slit lamp images of the control group (G), hydrogel group (H) and IOL group (I) at 3mo post-operation showed no significant corneal opacification, keratic precipitate or endophthalmitis. WPO: Week post-operation; MPO: Month post-operation; Yellow arrow: Hydrogel.
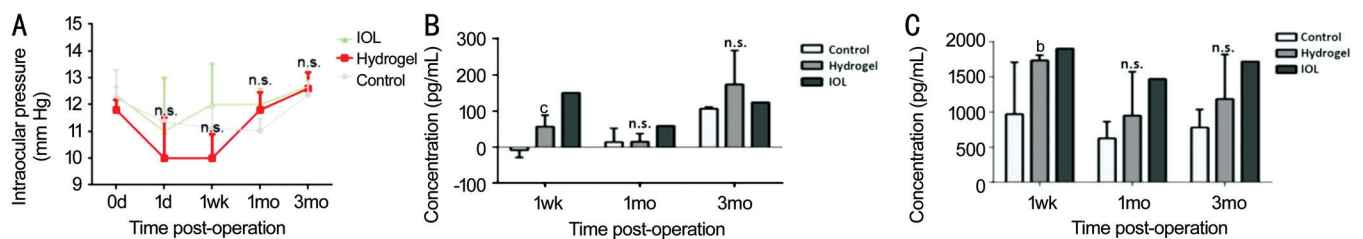

Figure 4 Effects of PAH implantation on the IOP and inflammatory factors in the aqueous humor A: The IOP recordings revealed no significant differences among the control, hydrogel and IOL groups; B-C: ELISA of inflammatory factors such as IL-8 (B) and TNF-α (C) in the aqueous humor of the control, hydrogel and IOL groups; Data are shown as the mean±SD. [b]$P<0.01$, [c]$P<0.005$. n.s.: No significance. Independent sample t-test.

hypopyon, or synechia was observed at 1mo post-operation among all the groups (Figure 3D-3F). Moreover, no anatomic abnormalities were observed at 3mo post-operation among all the groups (Figure 3G-3I). In addition, the alteration of IOP after hydrogel implantation was not statistically significant (Figure 4A). To further investigate the effect of PAH implantation on the intraocular inflammatory reaction, we performed ELISA to examine the key inflammatory factors IL-8 and TNF-α. ELISA of the aqueous humor showed that IL-8 (Figure 4B) and TNF-α (Figure 4C) of both the hydrogel and IOL groups were elevated at the first week post-operation, but that of the hydrogel group stayed consistent with that of the control group at 1 and 3mo post-operation. In sum,

implantation of the PAH did not induce any endophthalmitis in the New Zealand white rabbit eyes.

Effect of PAH Implantation on Visual Function Visual function may be well reflected by visual electrophysiology examinations, such as ERG. To further investigate the effect of PAH implantation on visual function, we conducted flash-ERG examinations of the control, hydrogel, and IOL groups. The amplitude of the a-wave of rod, cone and combined rod-cone (Max) ERG 3mo after hydrogel implantation was not significantly altered, nor was the peak time of the wave (Figure 5A, 5B). Similarly, both the amplitude and peak time of the b-wave of rod, cone and combined rod-cone (Max) ERG 3mo after hydrogel implantation were also not significantly altered
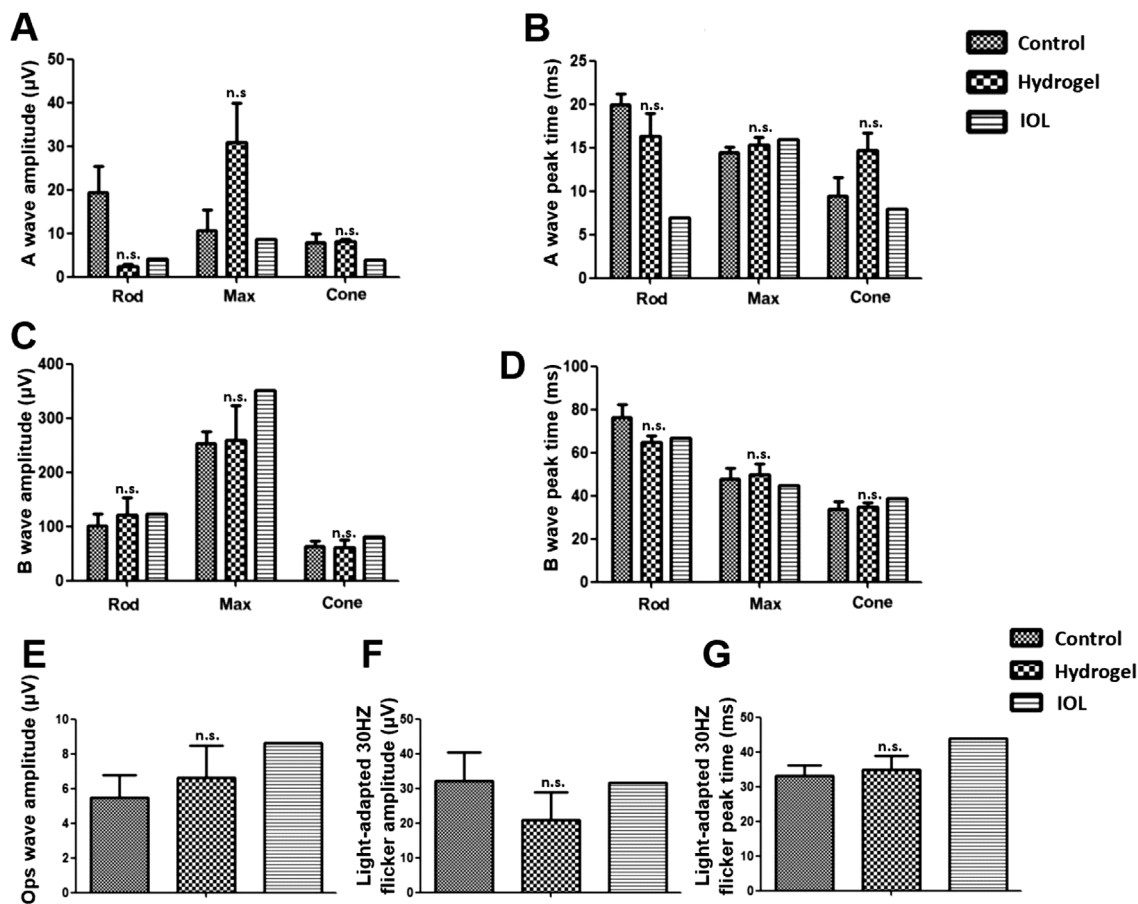
Figure 5 Flash-ERGs of New Zealand white rabbits at 3mo post-implantation A, B: Statistical analysis of the amplitudes (A) and peak time (B) of flash-ERG a-waves at 0.5 log(cd·s/m^2) in the three groups at 3mo post-operation; C, D: Statistical analysis of the amplitudes (C) and peak time (D) of flash-ERG b-waves at 0.5 log(cd·s/m^2) in the three groups at 3mo post-operation; E: Statistical analysis of the Ops wave amplitude at 3.0 log(cd·s/m^2) in the three groups at 3mo post-operation; F, G: Statistical analysis of the light-adapted 30 Hz flicker amplitude (F) and peak time (G) at 3.0 log(cd·s/m^2) in the three groups at 3mo post-operation; Data are shown as the mean±SD. n.s.: No significance. Independent sample *t*-test.

(Figure 5C, 5D). These results indicated normal function of photoreceptor cells and bipolar cells in the hydrogel groups 3mo post-operation. Moreover, we analyzed the characteristics of the Ops wave and light-adapted 30 Hz flicker. Consistent with the results above, the implantation of hydrogel did not affect the amplitude of the Ops wave and light-adapted 30 Hz flicker, as well as its peak time (Figure 5E-5G), indicating an intact and well-functioning inner retina and cone system.

Effect of PAH Implantation on Ocular Histology Novel biomaterials are often toxic to the ocular tissue and cause severe abnormalities in histology. To evaluate the effect of PAH implantation on the ocular histology, we first performed HE staining of New Zealand white rabbit eyes after 3mo of surgery. This result indicated that the hydrogel group maintained its normal histological characteristics, such as cell connections and layered lamination, as well as did the IOL group, all compared with the control group (Figure 6). The TUNEL assay revealed that no cellular apoptosis emerged at the cornea, anterior chamber angle (ACA), or retina in any of the three groups,

confirming the nontoxic character of the PAH (Figure 7J-7R). Moreover, IBA1$^+$ macroPAHge cells did not accumulate in the cornea or retina except for the ACA in the hydrogel and IOL groups 3mo post-implantation (Figure 7A-7I). The recruitment of macroPAHges at the ACA may represent the immune response caused by the hydrogel or IOL implants, which triggered the PAHgocytic activation of macroPAHges.

DISCUSSION

The eye exerts a unique ocular morphology, and all ocular organic architectures are susceptible to a number of diseases that may require treatment *via* different modalities, such as sustained drug delivery and artificial bio tissue substitution[17]. In the past century, hydrogels have been used in various applications as effective materials. The unique network structure of a hydrogel makes it highly hydrophilic and biocompatible, and it exhibits soft physical properties similarly to living tissue, which makes it an ideal and potential biomaterial for ophthalmic applications such as intraocular pumps, injections and implants, reducing comorbidities
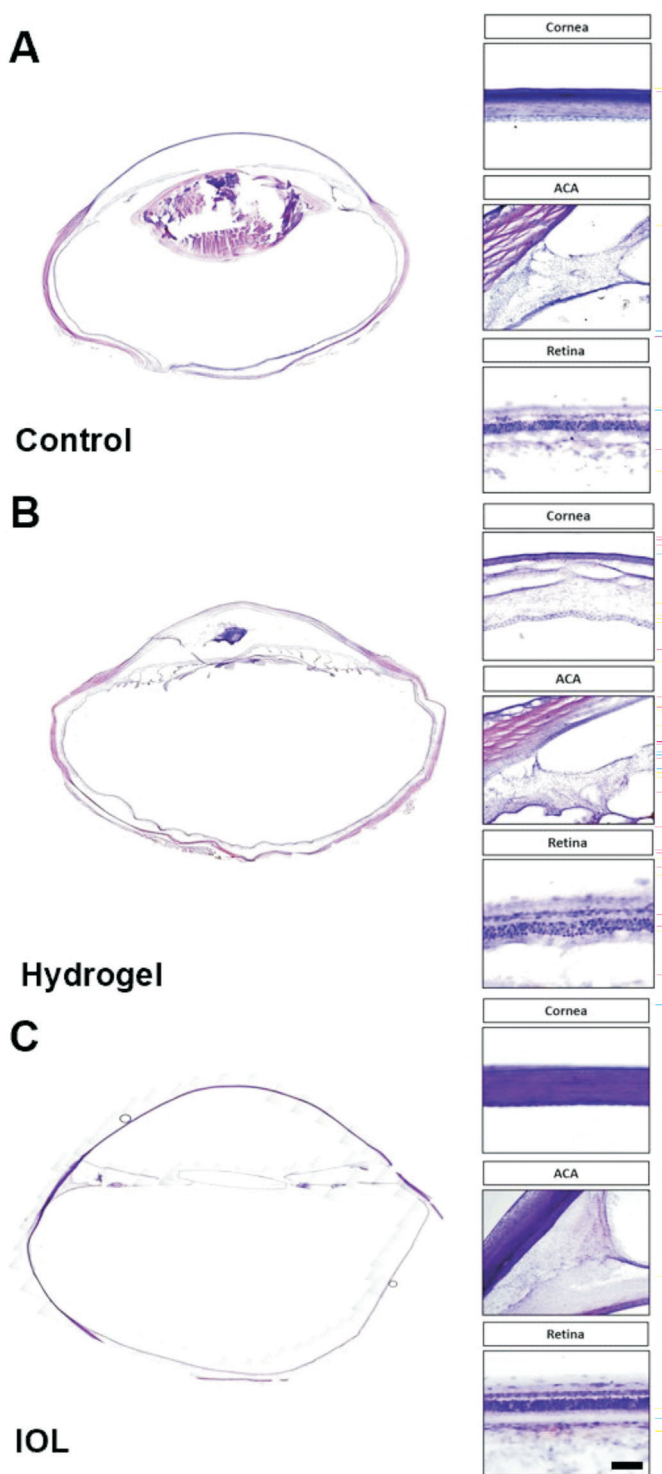
Figure 6 The PAH does not cause histological alteration 3mo post-implantation HE staining of New Zealand white rabbit eyes showed the detailed histological identity of the cornea, ACA, and retina in the control (A), hydrogel (B), and IOL (C) group. The cell connectivity and layered lamination in hydrogel group were normal compared with those of control group; the cornea was ruptured due to the limitations of HE staining procedure. Scale bar, 100 μm.

caused by glaucoma, cataracts, and diabetic retinopathies[18]. 3D printing allows the creation of objects with complex 3D geometries and photologies from a computer-aided design and printed biomaterials to tissue analog structures without any change in their mechanical or biological properties[19-20]. However, given the nature of the polymers in hydrogel formulations and the materials used in the preparation of ophthalmic gels, it is paramount that any new hydrogel formulation intended for ocular application should be inevitably investigated for potential toxicity/adverse effects on ocular tissues. In this report, we generated a PAH as a thin film and found that the newly formed hydrogel needs 9d of pretreatment with PBS to stabilize its structure, reflecting the stimuli-controlled PAHse transition and small molecule release characteristics of stimulus-responsive hydrogels[21]. We performed coculture experiments *in vitro* and implantation experiments *in vivo* to assess the effect of the hydrogel on ocular tissue. The biosafety research parameters for structure, function, and inflammation, such as cell proliferation assays, inflammation detection by slit lamp and aqueous humor tests, visual function assay by ERG, and anatomical abnormality detection by HE staining and immunostaining, indicated that the PAH is qualified as a biosafe clinical-grade biomaterial for 3D-printed IOLs by systematic investigation and verification both *in vivo* and *in vitro*.

The polymers in preformed ophthalmic hydrogels could be semisynthetic or natural. Some of them can transit from sol to gel conversely triggered by environmental stimuli such as temperature, pH and ion concentration[10,22]. As the PAH was primarily performed by 3D printing, it was harmful to cell proliferation when co-cultured with LECs. However, pretreatment of the PAH with PBS for 9d robustly reduced the toxic effect to LECs. This result indicated two points of view: first, the primary PAH could respond to the cell culture environment conditions and release polymers that inhibit cellular proliferation at a high concentration; second, adaptation to the extracellular environment is needed and should be properly investigated and standardized for the safe clinical use of PAHs.

When co-cultured with the PAH, both LECs and ARPE19 cells exhibit contact cell death, while cells located far away from the hydrogel grow without any abnormalities. Cell migration and proliferation are highly dependent on the extracellular matrix[23]. To serve as an ideal environment and matrix, ophthalmic hydrogels must be composed of gelatin[24], alginate[25], collagen[26], fibrin[27], and even molecularly modified biomaterials. 3D-printed IOLs have a high light transparency but may be populated by migratory and proliferative cells[28-29]. The contact cell death of the PAH prevented this possibility of this adverse effect of cell migration and proliferation, which makes it an ideal transparent biomaterial with the least opacity after IOL implantation.

A previous study on the ocular tolerability of a new biomaterial formulation used the "Draize rabbit eye irritation test" which
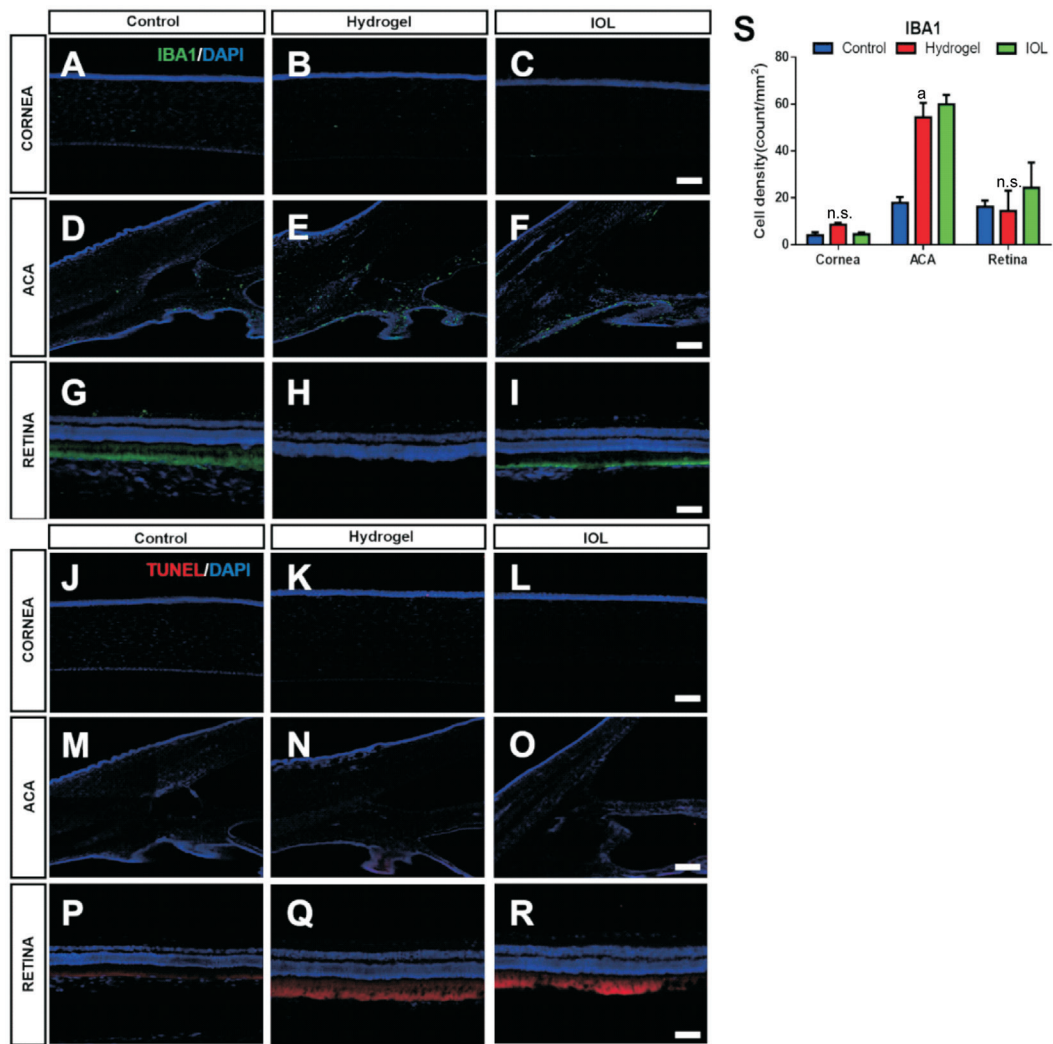
Figure 7 Macrophage activation and cell apoptosis of New Zealand white rabbit eyes 3mo after PAH implantation A-I: Immunostaining of Iba1 in New Zealand white rabbit eyes at 3mo post-implantation showed Iba1^{+} macrophage augmentation at the cornea (A-C), ACA (D-F) and retina (G-I) in the control group (A, D, G), the hydrogel group (B, E, H), and the IOL group (C, F, I); J-R: TUNEL assay of New Zealand white rabbit eyes at 3mo post-implantation showed TUNEL[+] apoptotic cell accumulation at the cornea (J-L), ACA (M-O) and retina (P-R) in the control group (J, M, P), the hydrogel group (K, N, Q), and the IOL group (L, O, R); S: Statistical analysis of Iba1^{+} macrophages in the cornea, ANA, and retina in all three groups. Scale bar, 100 μm. Data are shown as the mean±SD. [a]P<0.05. n.s.: No significance. Independent sample t-test.

is the oldest and most classic test that has been employed to evaluate potential ocular irritation. However, the Draize test is quite limited by its subjectivity, poor reproducibility and the need for large numbers of live rabbits[30-31]. In the current research, we utilized ELISA to explore the inflammatory factor level of the aqueous humor, and we conducted ERG analyses to examine the visual function after hydrogel implantation. These analyses well addressed the shortcomings of the Draize test and provided distinguished data to gain insight into the effect on ocular inflammation and visual function.

MacroPAHges are a type of immune cell that engulfs and digests debris, foreign substances, and microbes[32]. They are patrol guards in the microenvironment of all tissues, which are transformed into active PAHgocytes by morphology and function and react quickly to various kinds of tissue damage. There is conclusive evidence in animal models and in situ

analysis of human tissues that the macroPAHge response is a common feature of various retinal inflammatory diseases[33-37]. We found accumulated Iba1^{+} macroPAHges in the ACA and iris of both hydrogel groups 3mo post-operation. The morphology of Iba1^{+} macroPAHges in the ACA and iris is ameboid like, suggesting that the PAHgocytic amoeboid movement of emerging macroPAHges is triggered by hydrogel implantation. Most importantly, we found similar results in the IOL group, which served as a positive biosafe control group, and no corneal opacity, keratic precipitate, hypopyon, or synechia were observed in the hydrogel or IOL group.

As the implanted IOL will be left in the eye for several years after surgery, there is growing interest in the use of IOLs as drug reservoirs or as treatment methods for ophthalmic diseases. Combining 3D printing technology and the biocompatible PAH as the printing material, as well as a

potential material for stimuli-responsive hydrogel fabrication, we hold the possibility of loading antibiotics, corticosteroids, and non-steroidal anti-inflammatory drugs in the IOL, which integrates cataract surgery and postoperative treatments as a one-step procedure[38]. Moreover, IOLs can also be incorporated with telescopic lenses, presbyopia-correcting lenses, or accommodative polyfocal bio analogical lenses[39-40]. These advanced designs could become more effective and personalized when combined with 3D printing and biocompatible hydrogels. However, all these IOLs inevitably require rigid biosafety assessments and more clinical studies to ascertain their safety and effectiveness.

In sum, the implantation of the PAH did not disturb the IOP, blood parameters, ERG or optical structure, indicating that it will not cause any ocular irritation. However, it is not clear whether this hydrogel lens maintains the nano smooth surface, which can hopefully to correct visual errors, including the defocusing and astigmatism caused by traditional IOLs. We will improve the manufacturing process in the future and test the correction capacity of this new lens in terms of visual quality. Our research provides insight into the biosafety of PAHs in ocular tissue and demonstrates that PAHs are a safe material for 3D printing of personal IOLs, which hold great potential for future clinical applications.

ACKNOWLEDGEMENTS

REFERENCES

1 Liu YC, Wilkins M, Kim T, Malyugin B, Mehta JS. Cataracts. *Lancet* 2017;390(10094):600-612.

2 Allen D, Vasavada A. Cataract and surgery for cataract. *BMJ* 2006;333(7559):128-132.

3 Kim TI, Alió Del Barrio JL, Wilkins M, Cochener B, Ang M. Refractive surgery. *Lancet* 2019;393(10185):2085-2098.

4 Zopf DA, Hollister SJ, Nelson ME, Ohye RG, Green GE. Bioresorbable airway splint created with a three-dimensional printer. *N Engl J Med* 2013;368(21):2043-2045.

5 Atala A, Bauer SB, Soker S, Yoo JJ, Retik AB. Tissue-engineered autologous bladders for patients needing cystoplasty. *Lancet* 2006;367(9518):1241-1246.

6 Isaacson A, Swiokla S, Connon CJ. 3D bioprinting of a corneal stroma equivalent. *Exp Eye Res* 2018;173:188-193.

7 Sommer AC, Blumenthal EZ. Implementations of 3D printing in ophthalmology. *Graefes Arch Clin Exp Ophthalmol* 2019;257(9): 1815-1822.

8 Debellemanière G, Flores M, Montard M, Delbosc B, Saleh M. Three-dimensional printing of optical lenses and ophthalmic surgery: challenges and perspectives. *J Refract Surg* 2016;32(3):201-204.

9 Shiblee MNI, Ahmed K, Khosla A, Kawakami M, Furukawa H. 3D printing of shape memory hydrogels with tunable mechanical properties. *Soft Matter* 2018;14(38):7809-7817.

10 Al-Kinani AA, Zidan G, Elsaid N, Seyfoddin A, Alani AWG, Alany RG. Ophthalmic gels: Past, present and future. *Adv Drug Deliv Rev* 2018;126:113-126.

11 Hinze U, El-Tamer A, Reiß S, Stolz H, Guthoff R, Stachs O, Chichkov B. Implantatdesign mittels multiphotonen-polymerisation. *Klin Monatsbl Augenheilkd* 2015;232(12):1381-1385.

12 Chen X, Chen ZH, Li ZY, Zhao C, Zeng YX, Zou T, Fu CY, Liu XL, Xu HW, Yin ZQ. Grafted c-kit[+]/SSEA1^{-} eye-wall progenitor cells delay retinal degeneration in mice by regulating neural plasticity and forming new graft-to-host synapses. *Stem Cell Res Ther* 2016;7(1):191.

13 Ullrich M, Aßmus B, Augustin AM, Häbich H, Abeßer M, Martin Machado J, Werner F, Erkens R, Arias-Loza AP, Umbenhauer S, Wagner H, Benz PM, Unger A, Linke WA, Frantz S, Baba HA, Kuhn M, Schuh K. SPRED2 deficiency elicits cardiac arrhythmias and premature death via impaired autoPAHgy. *J Mol Cell Cardiol* 2019;129:13-26.

14 Lyu XM, Ma YQ, Wu F, Wang L, Wang LN. LncRNA NKILA inhibits retinoblastoma by downregulating lncRNA XIST. *Curr Eye Res* 2019;44(9):975-979.

15 Yu X, Shen N, Zhang ML, Pan FY, Wang C, Jia WP, Liu C, Gao Q, Gao X, Xue B, Li CJ. Egr-1 decreases adipocyte insulin sensitivity by tilting PI$_3$K/Akt and MAPK signal balance in mice. *EMBO J* 2011;30(18):3754-3765.

16 Liu WY, Liu MM, Liu Y, Li SY, Weng CH, Fu Y, He JC, Gong Y, Liu WP, Zhao CJ, Yin ZQ. Validation and safety of visual restoration by ectopic expression of human melanopsin in retinal ganglion cells. *Hum Gene Ther* 2019;30(6):714-726.

17 Patel A, Cholkar K, Agrahari V, Mitra AK. Ocular drug delivery systems: an overview. *World J PAHrmacol* 2013;2(2):47-64.

18 Koetting MC, Peters JT, Steichen SD, Peppas NA. Stimulus-responsive hydrogels: theory, modern advances, and applications. *Mater Sci Eng R Rep* 2015;93:1-49.

19 Norman J, Madurawe RD, Moore CM, Khan MA, Khairuzzaman A. A new chapter in PAHrmaceutical manufacturing: 3D-printed drug products. *Adv Drug Deliv Rev* 2017;108:39-50.

20 Huang W, Zhang X. 3D Printing: print the future of ophthalmology. *Invest Ophthalmol Vis Sci* 2014;55(8):5380-5381.

21 Willner I. Stimuli-controlled hydrogels and their applications. *Acc Chem Res* 2017;50(4):657-658.

22 Craig JP, Singh I, Tomlinson A, Morgan PB, Efron N. The role of tear physiology in ocular surface temperature. *Eye (Lond)* 2000;14(Pt 4):635-641.

23 Cope EC, Gould E. Adult neurogenesis, glia, and the extracellular matrix. *Cell Stem Cell* 2019;24(5):690-705.

24 Billiet T, Gevaert E, De Schryver T, Cornelissen M, Dubruel P. The 3D printing of gelatin methacrylamide cell-laden tissue-engineered constructs with high cell viability. *Biomaterials* 2014;35(1):49-62.

25 Duan B, Hockaday LA, Kang KH, Butcher JT. 3D bioprinting of heterogeneous aortic valve conduits with alginate/gelatin hydrogels. *J Biomed Mater Res A* 2013;101(5):1255-1264.

26 Mazzocchi A, Devarasetty M, Huntwork R, Soker S, Skardal A. Optimization of collagen type I-hyaluronan hybrid bioink for 3D bioprinted liver microenvironments. *Biofabrication* 2018;11(1):015003.

27 Lee YB, Polio S, Lee W, Dai GH, Menon L, Carroll RS, Yoo SS. Bio-printing of collagen and VEGF-releasing fibrin gel scaffolds for neural stem cell culture. *Exp Neurol* 2010;223(2):645-652.

28 Buwalda SJ, Vermonden T, Hennink WE. Hydrogels for therapeutic delivery: current developments and future directions. *Biomacromolecules* 2017;18(2):316-330.

29 Wu ZJ, Su X, Xu YY, Kong B, Sun W, Mi SL. Bioprinting three-dimensional cell-laden tissue constructs with controllable degradation. *Sci Rep* 2016;6:24474.

30 Lordo RA, Feder PI, Gettings SD. Comparing and evaluating alternative (in vitro) tests on their ability to predict the Draize maximum average score. *Toxicol In Vitro* 1999;13(1):45-72.

31 Abdelkader H, Ismail S, Hussein A, Wu ZM, Al-Kassas R, Alany RG. Conjunctival and corneal tolerability assessment of ocular naltrexone niosomes and their ingredients on the hen's egg chorioallantoic membrane and excised bovine cornea models. *Int J PAHrm* 2012;432(1-2):1-10.

32 Ovchinnikov DA. MacroPAHges in the embryo and beyond: much more than just giant PAHgocytes. *Genesis* 2008;46(9):447-462.

33 Karlstetter M, Scholz R, Rutar M, Wong WT, Provis JM, Langmann T. Retinal microglia: just bystander or target for therapy? *Prog Retin Eye Res* 2015;45:30-57.

34 Rathnasamy G, Foulds WS, Ling EG, Kaur C. Retinal microglia--A key player in healthy and diseased retina. *Prog Neurobiol* 2019;173:18-40.

35 Kanazawa H, Ohsawa K, Sasaki Y, Kohsaka S, Imai Y. MacroPAHge/microglia-specific protein Iba1 enhances membrane ruffling and Rac activation via phospholipase C-gamma -dependent pathway. *J Biol Chem* 2002;277(22):20026-20032.

36 Okayasu T, Quesnel AM, O'Malley JT, Kamakura T, Nadol JB Jr. The distribution and prevalence of macroPAHges in the cochlea following cochlear implantation in the human: an immunohistochemical study using anti-Iba1 antibody. *Otol Neurotol* 2020;41(3):e304-e316.

37 Cora MC, Janardhan KS, Jensen H, Clayton N, Travlos GS. Previously diagnosed reticulum cell hyperplasia in decalcified rat bone marrow stain positive for ionized calcium binding adapter molecule 1 (Iba1): a monocytic/macroPAHge cell marker. *Toxicol Pathol* 2020;48(2):317-322.

38 Liu YC, Wong TT, Mehta JS. Intraocular lens as a drug delivery reservoir. *Curr Opin Ophthalmol* 2013;24(1):53-59.

39 Boyer D, Freund KB, Regillo C, Levy MH, Garg S. Long-term (60-month) results for the implantable miniature telescope: efficacy and safety outcomes stratified by age in patients with end-stage age-related macular degeneration. *Clin Ophthalmol* 2015;9:1099-1107.

40 Ford J, Werner L, Mamalis N. Adjustable intraocular lens power technology. *J Cataract Refract Surg* 2014;40(7):1205-1223.